

## Phase transitions and oscillations in a lattice prey-predator model

Tibor Antal and Michel Droz

*Département de Physique Théorique, Université de Genève, CH 1211 Genève 4, Switzerland*

(Received 29 September 2000; revised manuscript received 8 February 2001; published 20 April 2001)

A coarse grained description of a two-dimensional prey-predator system is given in terms of a simple three-state lattice model containing two control parameters: the spreading rates of prey and predator. The properties of the model are investigated by dynamical mean-field approximations and extensive numerical simulations. It is shown that the stationary state phase diagram is divided into two phases: a pure prey phase and a coexistence phase of prey and predator in which temporal and spatial oscillations can be present. Besides the usual directed percolationlike transition, the system exhibits an unexpected, different type of transition to the prey absorbing phase. The passage from the oscillatory domain to the nonoscillatory domain of the coexistence phase is described as a crossover phenomena, which persists even in the infinite size limit. The importance of finite size effects are discussed, and scaling relations between different quantities are established. Finally, physical arguments, based on the spatial structure of the model, are given to explain the underlying mechanism leading to local and global oscillations.

DOI: 10.1103/PhysRevE.63.056119

PACS number(s): 05.70.Ln, 64.60.Cn, 87.10.+e

### I. INTRODUCTION

The dynamics of interacting species has attracted a great deal of attention, since the pioneering works of Lotka [1] and Volterra [2]. In their independent studies, they showed that simple prey-predator models may exhibit limit cycles during which the populations of both species have periodic oscillations in time. However, this behavior depends strongly on the initial state, and is not robust to the addition of more general nonlinearities or to the presence of more than two interacting species [3]. In many cases the system reaches a simple steady state.

A better understanding of the properties of such oscillations is clearly desirable, as population cycles are often observed in ecological systems, and the underlying causes remain a long-standing open question [4]. One of the best documented examples concerns the Canadian lynx population. This population was monitored for more than 100 years (starting in 1820) from different regions of Canada. It was observed that the population oscillates with a period of approximately ten years, and that this synchronization was spatially extended over areas of several millions of square kilometers [5]. Several attempts were made to explain these facts (climatic effects, relations with the food-web, influence of the solar cycle) without success. More recently, Blasius *et al.* [4] introduced a deterministic three level vertical food-chain model. The three coupled nonlinear differential equations defining the model contain eight free parameters and two unknown nonlinear functions. The authors showed that an *ad hoc* choice of the free parameters and nonlinear functions explains the experimental data for the Canadian lynx.

In such mean-field type models, it is assumed that the populations evolve homogeneously, which is obviously an oversimplification. An important question consists of understanding the role played by the local environment on the dynamics [6]. There are many examples in equilibrium and nonequilibrium statistical physics showing that, in low enough dimensions, the local aspects (fluctuations) play a crucial role and have some dramatic effects on the dynamics

of the system. Accordingly, a great deal of activity has been devoted in the last few years to the study of extended prey-predator models [7]. The simplest spatial generalizations are the so called two patch models, where the species follow the conventional prey-predator rules within each patch, and can migrate from one patch to the other [8].

Other works have found that the introduction of stochastic dynamics plays an important role [9], as well as the use of discrete variables, which prevent the population from becoming vanishingly small. These ingredients are included in so called individual based lattice models, for which each lattice site can be empty or occupied by one [10–14] individual of a given species or two [15,16] individuals belonging to different species. It was recognized that these models give a better description of the oscillatory behavior than the usual Lotka-Volterra (LV) equations. Indeed, the oscillations in such finite size lattice models are stable against small perturbations of the prey and predator densities, and they do not depend on the initial state. It was also found (in two-dimensional systems) that the amplitude of the oscillations of global quantities decreases with increasing system size, while the oscillations persist on a local level. It was argued that coherent periodic oscillations are absent in large systems (although, the authors of Ref. [10] did not discard this possibility). In Ref. [15] Lipowski stated that this is only possible in three dimensions. In Ref. [12] Provata *et al.* emphasized that the frequency of the oscillations are stabilized by the lattice structure, and that it depends on the lattice geometry. In some papers, the stationary phase diagram was also derived for a given system size [10,16], and different phases were observed as functions of the model parameters, such as an empty phase, a pure prey phase, and an oscillatory region of coexisting prey and predator. In Ref. [10], a coexistence region without oscillations and a domain of the control parameter space for which the stationary states depend strongly upon the initial condition, were also found.

However, in all the above works no systematic finite size studies were performed, allowing one to draw firm conclusions about the phase diagram of the models as a function of

their sizes. In particular, the size dependence of the amplitude of the oscillations, as well as a detailed description of the critical behavior near the phase transitions, were not investigated. However, it is known [17] that, in ecological problems, the fact that a system has a finite size is more relevant than in most of the cases encountered in statistical physics, for which one concentrates on the thermodynamic limit. Another relevant question concerns the generic properties of such models.

The goal of this paper is to study a simple prey-predator model on a two-dimensional lattice, for which some of the above questions could be answered. Our model is based on a coarse-grained description in the sense that a given cell models a rather large part of a territory, and thus can contain many preys or predators. Moreover, predators cannot live without prey in a given cell. Those are the main differences between our model and that of Satulovsky and Tomé (ST) [10]. Nevertheless, it turns out that the stationary state phase diagram of the two models are quite different.

Our model is defined in Sec. II. Although governed by only two control parameters, this model exhibits a rich phase diagram. Two different phases are observed: a pure prey phase (P), and a coexistence phase of prey and predator in which an oscillatory (O) region and a nonoscillatory (NO) region can be distinguished. In some limiting cases the model can be mapped onto a well known nonequilibrium model: the *contact process* (CP) [18]. In Sec. III the properties of our model are analyzed in dynamical one- and two-point mean-field approximations, and no undamped oscillatory behavior is found. In Sec. IV, extensive Monte Carlo (MC) simulations are performed. It is shown that, as a function of the values of the control parameters, a usual directed percolation (DP) transition, as well as an unexpected transition belonging to a different universality class, into a prey absorbing state are present. The system size dependence of the amplitude of the oscillations is studied, and several scaling relations between the amplitude of the oscillations and the correlation length are obtained. In Sec. V an underlying mechanism responsible for the spatial oscillations is proposed, which leads to a qualitative explanation of the properties of the phase diagram. In particular, we show that the spatially extended aspect of the model plays a crucial role in the presence of oscillations. Finally, conclusions are drawn in Sec. VI.

## II. MODEL

Our system models prey and predator living together in a two-dimensional territory. This territory is divided into square cells, and each of them can contain several prey and predators. In this coarse-grained description, in which each cell represents a rather large territory, one can assume that each cell containing some predator will also contain some prey. Note that similar assumptions have been used in host-parasite models [19]. Here, we consider a three state representation. Each cell of a two-dimensional square lattice (of size  $L \times L$ , with periodic boundary condition), labeled by the index  $i$ , can be, at time  $t$ , in one of the three following states:  $\sigma_i = 0, 1$ , and  $2$ . A cell in a state  $0, 1$ , or  $2$  corresponds,

respectively, to a cell which is empty, a cell occupied by prey, or a cell occupied simultaneously by prey and predators. The dynamics of the system is defined as a continuous time Markov process. The transition rates for site  $i$  are (i)  $0 \rightarrow 1$  at rate  $\lambda_a(n_{i,1} + n_{i,2})/4$ , (ii)  $1 \rightarrow 2$  at rate  $\lambda_b(n_{i,2})/4$ , and (iii)  $2 \rightarrow 0$  at rate  $1$ , where  $n_{i,\sigma}$  denotes the number of nearest neighbor sites of  $i$  which are in the state  $\sigma$ .  $4$  is the coordination number of this two-dimensional square lattice.

The first two processes model the spreading of prey and predators. The two control parameters  $\lambda_a$  and  $\lambda_b$  characterize a particular prey-predator system. The reason for considering the sum  $n_{i,1} + n_{i,2}$ , in the first rule is simply that all the neighboring cells of  $i$  containing some prey (hence  $\sigma_i = 1$  or  $2$ ) will contribute to the prey repopulation of cell  $i$ . The third process represents the local depopulation of a cell due to overly greedy predators. This can be interpreted as the local extinction of a species, or as its migration to neighboring occupied sites. Spontaneous disappearance of a prey state ( $\sigma_i: 1 \rightarrow 0$ ), or that of the predators alone ( $\sigma_i: 2 \rightarrow 1$ ), is forbidden. These assumptions are reasonable because the occurrence of these processes is improbable. The rate of the third process is chosen to be  $1$ , which sets the time scale. As a consequence the time  $t$ , as well as  $\lambda_a$  and  $\lambda_b$ , is a dimensionless quantity.

The above dynamical rules are an extension of the contact process model [18,20] introduced as a description of epidemic spreading. The CP model is a two-state model,  $\sigma_i = 0, 1$ ; the states  $0$  and  $1$  represent healthy and infected individuals, respectively. The CP dynamical rules are (i)  $0 \rightarrow 1$  at rate  $\lambda(n_{i,1})/4$ , and (ii)  $1 \rightarrow 0$  at rate  $1$ . An epidemic survives for  $\lambda > \lambda_{CP}^* = 1.6488(1)$  [20], and disappears for  $\lambda < \lambda_{CP}^*$ . The transition toward this absorbing state is of second order and belongs to the DP universality class [20].

Our model differs from most of the lattice models previously investigated [10–13] in the fact that, on each site, each species may be represented by several individuals rather than just one. Our model, when suppressing the  $n_{i,2}$  term in the first rule, reduces to the ST model, in which the spreading rate of prey is simply proportional to the number of neighboring prey sites,  $n_{i,1}$ . Nevertheless, the presence of the  $n_{i,2}$  term in the first rule plays an important role, as we shall see below. The ST control parameters take the forms  $c = (1 + \lambda_a + \lambda_b)^{-1}$  and  $p = c(\lambda_b - \lambda_a)/2$ .

An interesting aspect of our model is its close relation to the CP model in some limiting cases. In the  $\lambda_a \rightarrow \infty$  limit the proportion of empty cells is negligible, since the empty cells are reoccupied by prey instantly after they become empty. Hence the lattice is completely covered by prey, and the  $\sigma = 2$  sites behave as the infected species in the CP model. That is, when decreasing  $\lambda_b$  the predator density decreases continuously and vanishes at the CP critical value  $\lambda_b^*(\lambda_a = \infty) = \lambda_{CP}^*$ .

One can think of the  $\lambda_b \rightarrow \infty$  limit in similar terms. In this case, the proportion of prey cells ( $\sigma = 1$ ) should be negligible due to the high productivity of predators, and the  $\sigma = 2$  cells should behave as the infected species in the CP among the empty cells. This is indeed the case if  $\lambda_a > \lambda_{CP}^*$ , but when  $\lambda_a$  becomes smaller than  $\lambda_{CP}^*$ , the prey density

again increases instead of becoming zero, as we shall see later.

### III. MEAN-FIELD ANALYSIS

Although apparently simple, there is no way to solve the model defined above analytically. However, analytical solutions can be obtained by making some approximations. The simplest one is the one-point mean-field approximation, in which all spatial fluctuations are neglected. Thus the system is characterized by the (dimensionless) densities of prey,  $a$ , and predator,  $b$ , sites,

$$a = \frac{1}{L^2} \sum_i (\delta_{\sigma_i,1} + \delta_{\sigma_i,2}), \quad b = \frac{1}{L^2} \sum_i \delta_{\sigma_i,2}, \quad (1)$$

whose values satisfy the  $0 \leq b \leq a \leq 1$  conditions by definition. In terms of these densities, the mean-field dynamical equations read

$$\frac{da}{dt} = \lambda_a a(1-a) - b \quad (2)$$

and

$$\frac{db}{dt} = \lambda_b b(a-b) - b. \quad (3)$$

Note that, for the  $b=0$  (and thus the  $a=0$ ) initial condition, the predator and prey densities remain 0.

Equations (2) and (3) clearly differ from the usual LV ones. The main difference lies in the interaction terms since, although a larger prey density increases the predator growth rate, the rate of predated preys only depends on the predator density. This is a simple consequence of the fact that there are no pure predator sites without preys in this model. This is reasonable for a real prey-predator system, as a predator has to consume a certain amount of prey in a given time to survive, independently of the number of preys around it. The  $(1-a)$  term in the first equation plays the role of a simple Verhulst factor, which assures an upper limit for the prey density ( $a \leq 1$ ), and similarly the  $(a-b)$  term in the second equation does not allow the density of predators to exceed that of the preys.

The stationary states are obtained by setting the left hand sides of Eqs. (2) and (3) to zero. Contrary to the simplest LV equations, qualitatively different stationary states are obtained varying the parameters,  $\lambda_a$  and  $\lambda_b$ , as illustrated in Fig. 1.

For  $0 \leq \lambda_b \leq 1$  and  $\lambda_a > 0$ , the stationary state is a pure prey absorbing state, where  $a^s = 1$  and  $b^s = 0$ . For  $\lambda_a = 0$  the stationary state is also a prey state,  $b^s = 0$ ; however, the value of  $a^s$  depends upon the initial state. In the rest of the plane ( $\lambda_a, \lambda_b$ ), the stationary solutions are

$$a^s = \frac{(\lambda_a - 1) + \sqrt{(\lambda_a - 1)^2 + 4\lambda_a/\lambda_b}}{2\lambda_a} \quad (4)$$

and

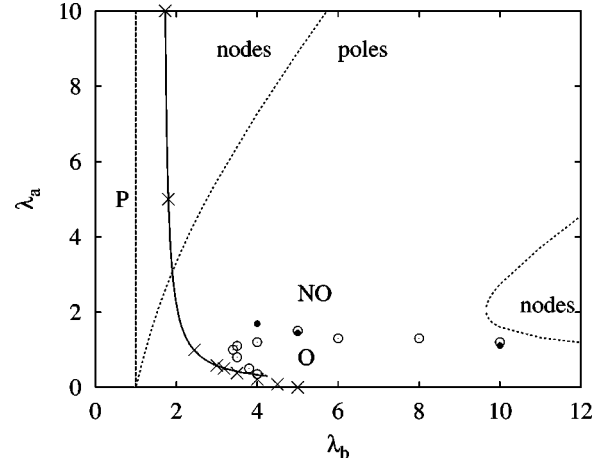


FIG. 1. Mean-field prediction for the boundary (dashed line) between the prey (P) and the coexistence phase (O and NO). The dotted lines are the boundaries between the pole and node type of stationary state regions. The MC results in the  $L \rightarrow \infty$  limit are also depicted for comparison (see Fig. 3 for details).

$$b^s = a^s - \frac{1}{\lambda_b}, \quad (5)$$

which describe a coexistence of prey and predators (coexistence phase).

For  $\lambda_b \gg 1$  the  $a$  and  $b$  densities are approximately the same,

$$a^s = b^s + O\left(\frac{1}{\lambda_b}\right) = \begin{cases} 1 - \frac{1}{\lambda_a} + O\left(\frac{1}{\lambda_b}\right) & \text{for } \lambda_a > 1 \\ O\left(\frac{1}{\sqrt{\lambda_b}}\right) & \text{for } \lambda_a = 1 \\ O\left(\frac{1}{\lambda_b}\right) & \text{for } \lambda_a < 1, \end{cases} \quad (6)$$

and, as a function of  $\lambda_a$ , they show a mean-field CP behavior, as expected from the argument given in Sec. II.

In the  $\lambda_a \gg 1$  limit (and for  $\lambda_b > 1$ ) the system is "full of prey," namely,

$$a^s = 1 - \frac{1}{\lambda_a} \left(1 - \frac{1}{\lambda_b}\right) + O\left(\frac{1}{\lambda_a^2}\right), \quad (7)$$

and the predator density reads

$$b^s = \left(1 - \frac{1}{\lambda_a}\right) \left(1 - \frac{1}{\lambda_b}\right) + O\left(\frac{1}{\lambda_a^2}\right). \quad (8)$$

As expected, its  $\lambda_b$  dependence agrees with the prediction of the mean-field approximation for the CP model. This approximation predicts a second order phase transition along the whole  $\lambda_b = 1$  line, as in the  $\lambda_b \rightarrow 1$  limit  $a$  and  $b$  approach linearly the values 1 and 0, respectively:

$$\begin{aligned}
a^s &= 1 - \frac{\lambda_b - 1}{\lambda_a + 1} + O[(\lambda_b - 1)^2], \\
b^s &= \lambda_a \frac{\lambda_b - 1}{\lambda_a + 1} + O[(\lambda_b - 1)^2].
\end{aligned} \tag{9}$$

The behavior of the densities is rather surprising at the  $\lambda_a = 0$  boundary of the coexistence phase. For  $0 < \lambda_a \ll 1$  and for  $\lambda_b > 1$ ,

$$a^s = \frac{1}{\lambda_b} + \lambda_a \left( \frac{1}{\lambda_b} + \frac{1}{\lambda_b^2} \right) + O(\lambda_a^2), \tag{10}$$

while the stationary solution  $a^s$  for  $\lambda_a = 0$  depends on the initial state. Thus the mean-field approximation predicts a discontinuity of the prey density along this boundary. However, the predator density  $b^s = a^s - \lambda_b^{-1}$  is proportional to  $\lambda_a$ , and thus continuous for  $\lambda_a \rightarrow 0$ .

Important quantities are the fluctuations of prey and predator densities (mean square deviations), which are normalized to become size independent for large systems,

$$\chi_\rho = L^2 \langle (\rho - \langle \rho \rangle)^2 \rangle, \quad \text{with } \rho = a \text{ or } b, \tag{11}$$

where  $\langle \rangle$  means the time average in the stationary state. For  $\lambda_a, \lambda_b \gg 1$  the majority of the sites are in a state 2, with a few holes in it, hence one can suppose that the holes are independent. Consequently, the number of the holes follows a Poisson distribution, from which the average hole number equals to the mean square deviation. There are  $L^2(1-a)$  holes made of sites in the state  $\sigma_i = 0$ , and  $L^2(1-b)$  holes made of sites in the states  $\sigma_i = 0$  or 1; thus

$$\chi_a \approx 1 - a^s \quad \text{and} \quad \chi_b \approx 1 - b^s. \tag{12}$$

These mean-field predictions are in good agreement with the simulations in a region (the nonoscillatory part) of the coexistence phase (see Fig. 9).

The stability of the stationary state can be analyzed by linear stability. One has to investigate the eigenvalues,  $\epsilon_{1,2}$ , of the Jacobian matrix related to the mean-field equations (2) and (3) at the stationary densities

$$\left( \begin{array}{cc} \partial_a \dot{a} & \partial_b \dot{a} \\ \partial_a \dot{b} & \partial_b \dot{b} \end{array} \right) \Big|_s = \left( \begin{array}{cc} \lambda_a(1 - 2a^s) & -1 \\ \lambda_b a^s - 1 & 1 - \lambda_b a^s \end{array} \right). \tag{13}$$

It turns out that the real parts of the eigenvalues are always negative, assuring the stability of the solutions. This mean-field approximation does not predict limit cycles, which would correspond to having an eigenvalue  $\epsilon$  with a zero real part. However, in some part of the coexistence phase the imaginary part is nonzero, so the stationary solution is approached in spirals (poles), instead of straight lines (nodes) (see Figs. 1 and 2), as also observed in the ST model [10]. Note that an unexpected node region appears for  $\lambda_b > 10$ . One can consider the presence of poles as an indication of the appearance of oscillations beyond the mean-field approximation. Note that, in this pole case, the damped oscillations

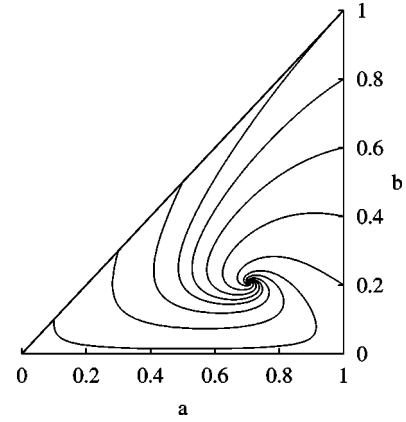


FIG. 2. Pole type approach for the stationary solution in the mean-field approximation for  $\lambda_a = 1$  and  $\lambda_b = 2$ , starting the system from different initial conditions. Note that the  $0 \leq b \leq a \leq 1$  conditions are always satisfied.

are strong along the  $\lambda_b$  axes (i.e., for  $\lambda_a \ll 1$ ). The strength of them can be characterized by the ratio of the imaginary and real parts of the eigenvalues, which have a singularity in the  $\lambda_a \rightarrow 0$  limit. Using Eq. (10), we obtain

$$\left| \frac{\text{Im}(\epsilon)}{\text{Re}(\epsilon)} \right| = 4\lambda_a^{-1/2} \sqrt{\lambda_b^2 - \lambda_b} + O(\lambda_a^{1/2}) \tag{14}$$

for  $\lambda_a \ll 1$  and  $\lambda_b > 1$ . In this limit one can also derive an expression for the frequency  $\omega$  of the damped oscillations:

$$\omega = |\text{Im}(\epsilon)| = 2\lambda_a^{1/2} \sqrt{1 - \frac{1}{\lambda_b}} + O(\lambda_a^{3/2}). \tag{15}$$

Thus the mean-field approximation predicts two distinct phases: the pure prey phase and the coexistence phase. It also gives some indications of the possible presence of oscillations in some parts of the coexistence phase. The boundaries of the two phases are described by two lines:  $\lambda_b = 1$  and  $\lambda_a = 0$ . Several quantities show a power-law behavior close to these boundaries, like  $b$  and  $1 - a$  at the  $\lambda_b = 1$  boundary, and  $b$  and  $\omega$  and the strength of the damped oscillations at the  $\lambda_a = 0$  boundary. Thus, in the mean-field approximation, the transitions are of second order, and the predator density  $b$  seems to be a good candidate for the order parameter. It goes to zero at the phase boundaries as  $b \sim (\lambda_b - 1)^\beta$  and  $b \sim \lambda_a^\beta$ , respectively, with a mean-field exponent  $\beta = 1$ .

We also performed a pair approximation, in which the nearest neighbor correlations were also considered as parameters. It turns out that the results differ only quantitatively from that of the one-point approximation. Contrary to Ref. [10], our system does not show a limit cycle behavior on the pair approximation level either.

#### IV. MONTE CARLO SIMULATIONS

On general grounds, one expects that fluctuations will play an important role in low dimensions. Our model is supposed to describe a two-dimensional world and, accordingly, we have performed extensive Monte Carlo simulations for

systems of sizes  $L \times L$ ,  $L$  varying between 100 and 1000. Concerning the boundaries of the system, one may think that open boundary conditions are the natural choice in view of biological interpretation. In this case, however, one has to introduce new dynamical rules at the boundaries which complicate the model. As it is known from the study of many problems in statistical mechanics, boundaries have important effects when they allow for a permanent current to flow through the system. We do not want to model such a case and, accordingly, we think that the periodic boundary conditions, which we use in the simulations, lead to a correct qualitative behavior. Note that similar boundary conditions have been used in the majority of previous works as well, which makes the comparison between the results easier.

Although our model is formulated as a continuous-time process, an equivalent (at least for not very short times) discrete time formulation is more suitable for numerical simulations. In one elementary time step one lattice site is chosen randomly, and its state evolves according to the rules defined in Sec. II using rescaled rates (all less than 1) as transition probabilities. One MC step is defined as the time needed such that all the sites are, on the average, visited once. In this paper we always use the original time units defined by the model, which can be obtained simply by rescaling the time measured in MC steps.

For sufficiently large system, the stationary state does not depend on the initial conditions. Usually we filled up the lattice completely with prey as an initial state, and put a few predators into it. To obtain the stationary phase diagram and the stationary values of the quantities of interest, from  $10^5$  to  $10^6$  MC steps were performed for systems of linear size  $L = 1000$  to 200 respectively.

The corresponding phase diagram, obtained for different system sizes, is depicted in Fig. 3. Two different phases are present as a function of the two control parameters  $\lambda_a$  and  $\lambda_b$ : a pure prey phase (P), a prey and predator coexistence phase with an oscillatory (O) region and a nonoscillatory (NO) region. In the oscillatory region, oscillations with a well defined frequency were observed in the prey and predator densities (see Fig. 4). A completely empty state would also be absorbing; however, during the simulations the system never reached such a state. A qualitative argument for this is simply that even one surviving prey can fill up the system with prey in the absence of predators. As Fig. 5 shows, the locations of the different regions of the phase space differ essentially from those obtained for the ST model.

The phase boundaries of the prey phase (see Fig. 3) were obtained in the following way. Simulations were started at parameter values for which the coexistence is maintained practically forever (up to the maximal number of MC steps investigated), and we decreased one of the parameter values by  $\Delta\lambda$ . If the predators were still alive after a given time  $\Delta t$ , we decreased the parameter further. The extinction of the predators defined the phase boundary.  $\Delta\lambda$  was chosen to be in the range 0.005 to 0.04, with  $\Delta t = 3 \times 10^4$  MC steps. The result was very similar, with  $\Delta t = 10^4$  and  $5 \times 10^4$  MC steps. The definition of the boundary between the oscillatory and

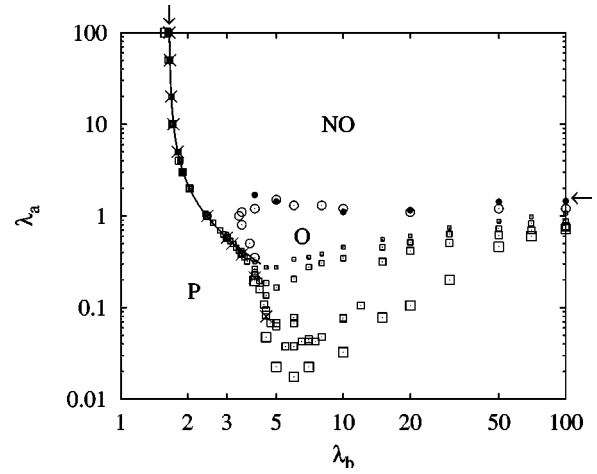


FIG. 3. Stationary state phase diagram as obtained by simulations. The squares ( $\square$ ) indicate the transition to the prey absorbing state (P) for different system sizes ( $L=100, 200, 500$ , and  $1000$ ), and the arrows point to the  $\lambda_b^*$  value. In all figures larger symbols correspond to larger systems. The boundary between the oscillatory (O) and the nonoscillatory (NO) regions of the coexistence phase is determined based on Fourier analysis ( $\circ$ ) and on the crossover in  $\chi_a$  ( $\bullet$ ). For the DP type transition between P and NO, the fitted values of  $\lambda_b^*(\lambda_a)$  ( $\times$ ) and the approximation described in Sec. V (solid line) are also depicted.

the nonoscillatory region of the coexistence phase will be described later.

In Fig. 3, the boundary of the prey phase is displayed for different system sizes ( $L=100, \dots, 1000$ ). Apparently, in the  $\lambda_a > \lambda_b$  regime the size dependence is negligible, but relevant for  $\lambda_a < \lambda_b$ . Note that this strong size dependence of the boundary coincides with the presence of oscillations.

Decreasing  $\lambda_b$  at any fixed value of  $\lambda_a$ , a second order phase transition takes place between the coexistence and the prey absorbing phases along a transition line  $\lambda_b^*(\lambda_a)$ . As for the mean-field case, the predator density is considered to be the order parameter. As  $\lambda_b \rightarrow \lambda_b^*(\lambda_a)$ , the order parameter  $b$  and  $1 - a$  go to zero as

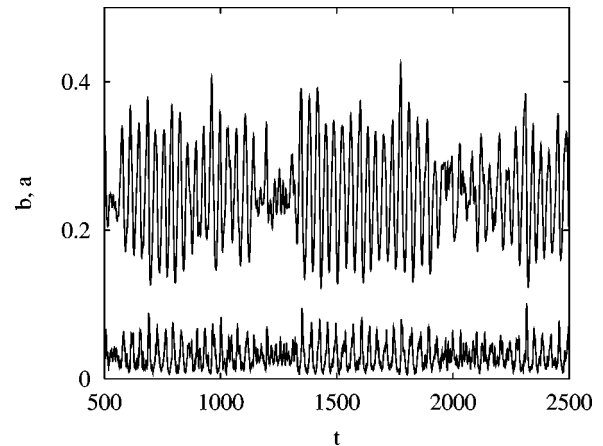


FIG. 4. Typical behavior of the prey,  $a$ , and the predator,  $b$  ( $b \leq a$ ), densities in the oscillatory region of the stationary state ( $\lambda_a = 0.8$ ,  $\lambda_b = 100$ , and  $L = 1000$ ).

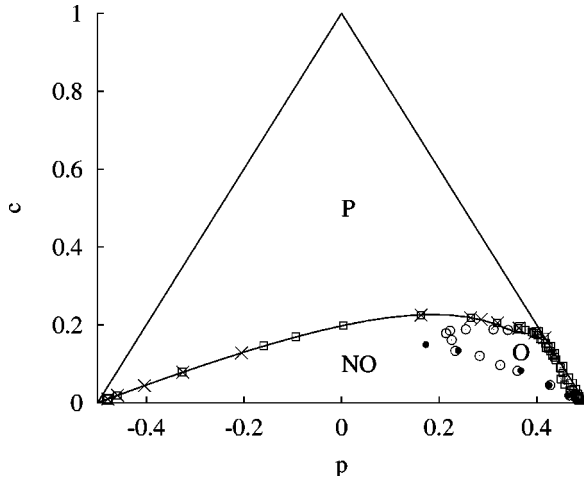


FIG. 5. The same as in Fig. 3, but as a function of the variables used in the ST model. The triangle represents the available part of the phase space. The location of the oscillatory (O) and nonoscillatory (NO) regions are quite different from that of the ST model.

$$b \sim 1 - a \sim [\lambda_b - \lambda_b^*(\lambda_a)]^{\beta_1}. \quad (16)$$

As seen in Fig. 3, the values of  $\lambda_b^*(\lambda_a)$  obtained by fitting the data with Eq. (16) are in very good agreement with the phase boundary obtained previously for large systems. Fitting the data leads to  $\beta_1 \approx 0.58(1)$  (with satisfactory precision for  $\lambda_a > 0.3$ ; see Fig. 6).

In the same limit the fluctuations of the predator density also follow a power-law behavior,  $\chi_b \sim [\lambda_b - \lambda_b^*(\lambda_a)]^{\gamma_1}$ . The exponent has been determined to a good precision as  $\gamma_1 \approx 0.35(3)$  for several values of  $\lambda_a$  between 1 and 50. The same behavior has been obtained (only for  $\lambda_a = 1$  and 3) for the prey fluctuations  $\chi_a$ , with the exponent  $\gamma_1 \approx 0.35(5)$ . The critical behavior turns out to be the same when the transition line is crossed while decreasing  $\lambda_a$  at fixed values of

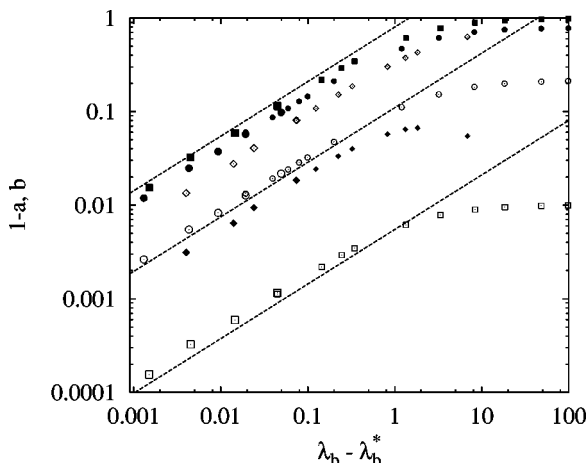


FIG. 6. Prey (open symbols) and predator (filled symbols) densities close to the second order phase transition line between the prey phase and the nonoscillatory region of the coexistence phase.  $\lambda_a = 0.5$  ( $\diamond$ ), 5 ( $\circ$ ), and 100 ( $\square$ ), while the system sizes are  $L = 200$  and 500. The slope of the dashed lines is the DP critical exponent  $\beta \approx 0.583$ .

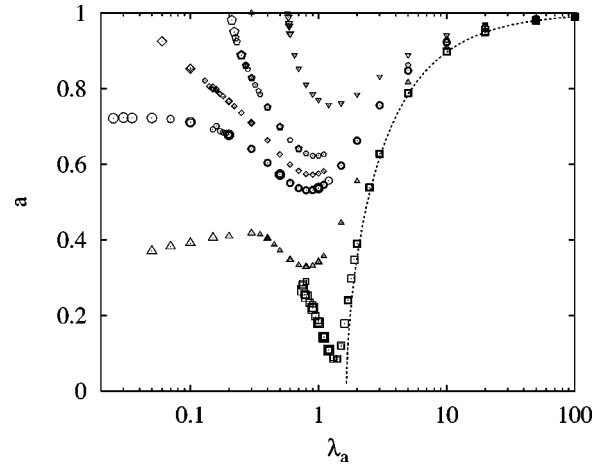


FIG. 7. Prey density  $a$  as a function of  $\lambda_a$  for different values of  $\lambda_b = 3$  ( $\nabla$ ), 4 (pentagon), 4.5 ( $\diamond$ ), 5 ( $\circ$ ), 10 ( $\triangle$ ), and 100 ( $\square$ ), and system sizes  $L = 200, 500$ , and 1000. The dashed line is the density given by the CP.

$\lambda_b$ . The two exponents,  $\beta_1$  and  $\gamma_1$ , are compatible with those obtained for DP in 2+1 dimensions [20]. Thus we conclude that this absorbing state phase transition belongs to the DP universality class, as expected on general grounds [21]. Note that a DP type phase transition in similar lattice prey-predator systems was already observed [16,22,23].

Let us now consider the limit  $L \rightarrow \infty$ . In this case, the phase diagram is rather simple, as can be seen in Fig. 1. A second order transition line  $\lambda_b^*(\lambda_a)$  separates the prey absorbing phase from the nonoscillatory coexistence phase. This line ends up at a particular point [ $\lambda_a = 0, \lambda_b^T \approx 5.0(3)$ ], where P, O, and NO domains meet. MC simulations suggest that the transition lines between the O and P domains observed for finite size systems collapse to the line  $\lambda_a = 0, \lambda_b > \lambda_b^T$  in the infinite size limit. This means that for this range of  $\lambda_b$ , and for any arbitrarily small  $\lambda_a$ , the coexistence of the species is possible providing that the system is large enough.

For  $\lambda_b > \lambda_b^T$ , when  $\lambda_a \rightarrow 0$ , the prey density  $a$  goes to a value smaller than 1 depending on  $\lambda_b$  (see Fig. 7). This differs from the DP transition case, where the prey density converges to 1. Moreover, according to the results depicted in Fig. 8, the predator density approaches zero as a power law,  $a \sim \lambda_a^{\beta_2}$  with  $\beta_2 \approx 1$ . Surprisingly, this situation is drastically different from the DP case, and the value  $\beta_2 \approx 1$  leads us to conjecture that this second transition could be mean-field-like. A complete analysis of the critical properties of the model near this transition line and the end point ( $\lambda_a = 0, \lambda_b = \lambda_b^T$ ) is a difficult task presently under investigation.

For  $\lambda_b > \lambda_b^T$  the fluctuations of the two densities  $\chi_a$  and  $\chi_b$  behave similarly. For a given  $\lambda_b$ , there is a clear crossover at  $\lambda_a^O(\lambda_b)$  from a mean-field-like behavior to a regime where the correlations are more important. For  $\lambda_a > \lambda_a^O(\lambda_b)$  the behavior of  $\chi_a$  and  $\chi_b$  agrees with that predicted by mean-field theory, reflecting the fact that in this range of  $\lambda_a$  the dominant behavior comes from the noise. Oscillations were observed in the overall densities in a region corresponding

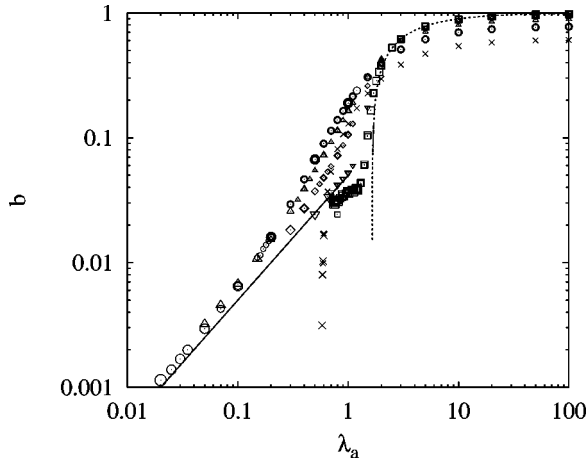


FIG. 8. Predator density  $b$  as a function of  $\lambda_a$  for different values of  $\lambda_b=3$  ( $\times$ ), 5 ( $\circ$ ), 10 ( $\triangle$ ), 20 ( $\diamond$ ), 50 ( $\nabla$ ), and 100 ( $\square$ ), and system sizes  $L=200, 500, 1000$ , and  $2000$  only for  $\lambda_b=5$ . The  $\lambda_a \rightarrow 0$  behavior is close to a power law with an exponent 1 (solid line), while the dashed line is the density given by the CP.

crudely to  $\lambda_a < \lambda_a^O(\lambda_b)$  (see Fig. 3). Thus the crossover point  $\lambda_a^O(\lambda_b)$  is taken as the definition of the border between the oscillatory and nonoscillatory regions.

After a proper normalization, the relative fluctuations collapse on a single curve for  $\lambda_a < \lambda_a^O(\lambda_b)$  (see Fig. 9). That is,

$$\frac{\chi_b}{b^2} \approx K_1(\lambda_b) \frac{\chi_a}{(1-a)^2}, \quad (17)$$

where the numerical factor  $K_1(\lambda_b)$  depends only on  $\lambda_b$ . However, the precision of the simulation was not good enough to obtain the functional form of  $K_1(\lambda_b)$  [neither of the forthcoming  $K_i(\lambda_b)$  for  $i=2, 3$ , and  $4$ ]. Nevertheless, Eq. (17) gives another size independent criterion to distinguish

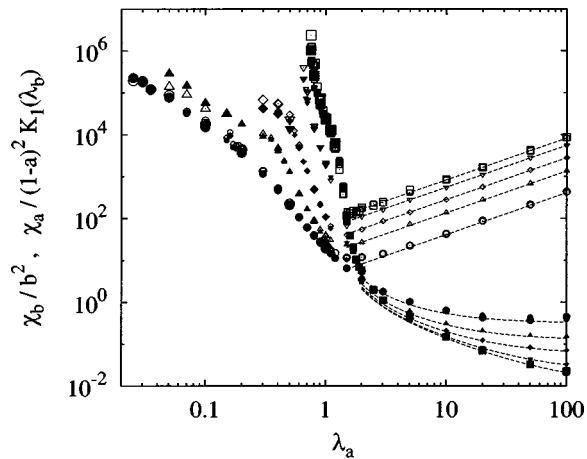


FIG. 9. Normalized (dimensionless) fluctuations of the prey (open symbols) and predator (filled symbols) densities,  $K_1(\lambda_b)\chi_a/(1-a)^2$  and  $\chi_b/b^2$ , which collapse in the oscillatory region. The parameters are  $\lambda_b=5$  ( $\circ$ ), 10 ( $\triangle$ ), 20 ( $\diamond$ ), 50 ( $\nabla$ ), and 100 ( $\square$ ), and system sizes  $L=200, 500$ , and  $1000$ . The dashed lines correspond to mean-field solutions (12).

between the oscillatory and nonoscillatory regions, as the relative fluctuations of prey and predator densities are proportional only in the oscillatory region.

The simulations showed that  $\chi_\rho$  ( $\rho=a$  or  $b$ ) is size independent, as expected from its definition [Eq. (11)]. As a consequence, the deviation from the average density,  $\sigma = \sqrt{\chi_\rho}/L$  [10], is smaller for larger systems and evidently scales with  $1/L$ . Certainly, this deviation increases with the intensity of oscillations. The above finite size behavior is in agreement with the results of earlier simulations, which claimed that the oscillations in the global densities disappear with increasing system size [11]. Our simulations predict more pronounced oscillations for smaller  $\lambda_a$  and larger  $\lambda_b$ .

The oscillations also have to show up in the correlation functions

$$C_a(i, \tau) = \langle (1 - \delta_{\sigma_j(t), 0})(1 - \delta_{\sigma_{j+i}(t+\tau), 0}) \rangle, \quad (18)$$

$$C_b(i, \tau) = \langle \delta_{\sigma_j(t), 2} \delta_{\sigma_{j+i}(t+\tau), 2} \rangle,$$

where  $j+i$  labels a lattice site a distance of  $i$  lattice spacing from the site  $j$ .  $C_\rho$  ( $\rho=a$  or  $b$ ) depends only on  $i$  and  $\tau$  due to the homogeneity of the system in space and time. For  $\tau=0$  the correlation function  $C_\rho(i)$ , obtained numerically, could be fitted by an exponential  $C_\rho(i) \sim \exp(-i/\xi_\rho)$ . In the oscillatory region the correlation lengths of preys and predators differ only through a  $\lambda_b$  dependent factor,  $\xi_a \approx K_2(\lambda_b)\xi_b$ , and they turned out to be proportional to the fluctuations of the prey density,  $\xi_a \approx \sqrt{2}\chi_a$ . This means that a more correlated system displays stronger oscillations. The reason for this is simply that the dynamics of the different sites show some synchronization within a correlation length, which results in larger oscillations (see Sec. V for more details).

In order to determine the characteristic frequency,  $\omega_\rho(\lambda_a, \lambda_b)$ , and the amplitude,  $A_\rho(\lambda_a, \lambda_b)$  ( $\rho=a$  or  $b$ ), of the oscillations, we measured the Fourier spectrum of the time dependent densities:

$$S_\rho(\omega) = \lim_{T \rightarrow \infty} \frac{1}{T} \left| \sum_{t=1}^T \rho(t) \exp(i\omega t) \right|^2. \quad (19)$$

The presence of oscillations is reflected as a peak at nonzero frequency in the Fourier spectrum. Extracting this peak from a background noise enables us to define  $A_\rho$  and  $\omega_\rho$  as the zeroth and first momenta of this distribution. This analysis clearly shows that the frequency of the oscillations is independent of the system size (see Fig. 10), and is the same for prey and predators. Moreover, for a wide range of the parameters in the oscillatory phase the frequency,  $\omega = \omega_a = \omega_b$ , is well approximated by  $\lambda_a/2$ . This linear behavior differs from the mean-field prediction.

In the oscillatory region the oscillations are present for arbitrarily large systems; however, their amplitude decreases with increasing system size, as  $1/L^2$ . At this point it is important to emphasize that this fact does not imply that only small oscillations are present in large systems. Indeed, for a large system the amplitude of the oscillations can be made

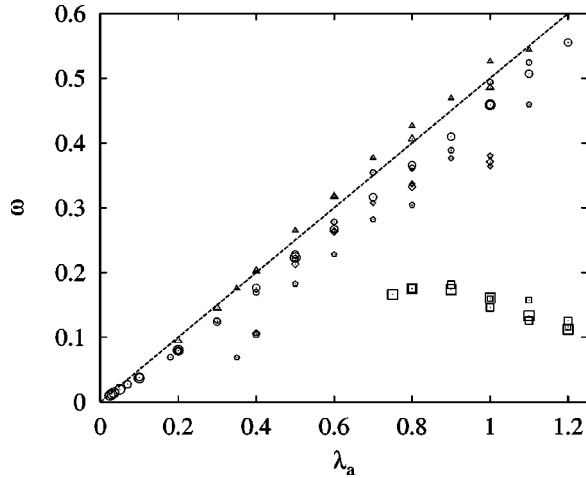


FIG. 10. Dimensionless frequency of the oscillations as a function of  $\lambda_a$  and for  $\lambda_b=4$  (pentagon), 5 ( $\circ$ ), 10 ( $\triangle$ ), 20 ( $\diamond$ ), and 100 ( $\square$ ) and for system sizes  $L=200, 500$ , and 1000. For a wide range of the parameters the data are close to  $\lambda_a/2$  (dashed line).

larger by decreasing  $\lambda_a$ . On the other hand, when increasing  $\lambda_a$  the amplitude goes to zero as a power law, which makes it difficult to define a phase boundary for the oscillations in this way. However, there is a simple scaling relation between the amplitude and the correlation length for the prey in the oscillatory region,

$$\xi_a^2 \approx 2\chi_a \approx L^2 A_a, \quad (20)$$

as can be observed in Fig. 11. The analogous expression for the predators is slightly more complicated,

$$\xi_b^2 \left( \frac{b}{1-a} \right)^2 K_3(\lambda_b) \approx \chi_b \approx K_4(\lambda_a) L^2 A_b, \quad (21)$$

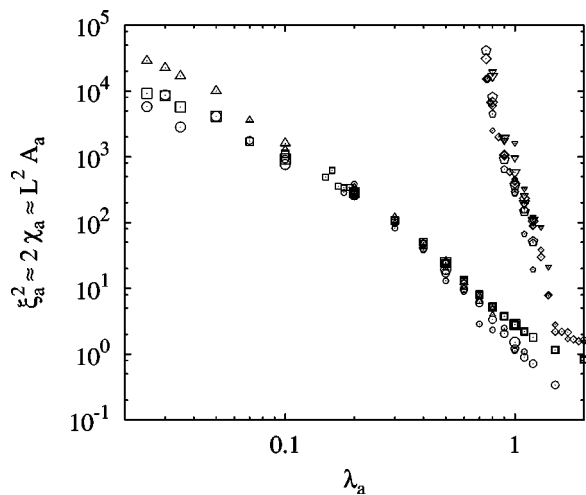


FIG. 11. Test of the relation between several (dimensionless) characteristics of the prey population [see Eq. (20)], namely, the correlation length  $\xi_a$  ( $\triangle, \nabla$ ), the fluctuations of the prey density,  $\chi_a$ , ( $\square, \diamond$ ), and the amplitude of the oscillations,  $A_a$  ( $\circ$ , pentagon) for  $\lambda_b=5$  and 100, respectively. The sizes of the system are  $L=200, 500$ , and 1000.

where  $K_3(\lambda_b)$  and  $K_4(\lambda_a)$  are numerical factors not given here.

Another quantity which characterizes the oscillations is the time dependent local correlations  $C_\rho(\tau) = C_\rho(i=0, \tau)$ . A similar investigation was made in Ref. [12] with time dependent correlations of the average local densities. In the oscillatory region  $C_\rho(\tau)$  displays damped, size independent oscillations. More precisely, the time correlations are size independent for any  $L > L_c(\lambda_a, \lambda_b)$ , while for any  $L < L_c$  the system evolves toward the prey absorbing state. Clearly, this critical system size is proportional to the correlation length  $L_c \sim \xi$ . The size independence of  $C(\tau)$  is a simple consequence of the fact that areas which are farther than  $\xi$  apart are uncorrelated. The investigation of the time dependent correlations, however, provides a rather ambiguous way to define the boundary of the oscillatory region. Indeed, one can observe local oscillations everywhere in the coexistence phase simply because, due to the cyclic dominance nature of the model, each site has to evolve in a loop ( $\sigma=0 \rightarrow 1 \rightarrow 2 \rightarrow 0 \dots$ ). Thus, according to the value of the damping factor, it is somehow arbitrary to decide whether a state is oscillatory or not.

It is worth noting that, at some particular values of  $\lambda_b$  ( $\lambda_b=10$  or 20) and for small  $\lambda_a$  values ( $\lambda_a < 0.2$  or 0.4, respectively), where the correlation length is comparable to the system size ( $L \sim 500$ ), the system can evolve to a stripe-like state. In this state three stripes of size  $L$ , made of predator, prey, and empty cells, drift through the system. However, for given  $\lambda_a$  and  $\lambda_b$  values, this behavior disappears when increasing the size of the system. The comparison of the MC results with the mean-field prediction shows that the latter gives a qualitatively correct description of the phase diagram (see Fig. 1), as well as of the discontinuity in the prey density,  $a$ , along the  $\lambda_a=0$  boundary.

## V. DISCUSSION

A qualitative understanding of the phase diagram is possible. If the birth rates are much larger than the death rate ( $\lambda_a \gg 1$  and  $\lambda_b \gg 1$ ), the system is full of prey and predators ( $a \approx b \approx 1$ ), while for small values of  $\lambda_b$  the system evidently reaches the pure prey absorbing state. As already discussed in Sec. II, in the  $\lambda_a \rightarrow \infty$  the system is full of prey ( $a \rightarrow 1$ ), and the predators behave like the infected species in the CP model. It means that they could survive only for  $\lambda_b > \lambda_{CP}^*$ , where a DP like second order transition occurs. This is in agreement with the mean-field results and with the simulation for  $\lambda_a=100$  (see Fig. 6).

One can also derive an approximate formula for the position of the phase boundary between the nonoscillatory phase and the prey phase  $\lambda_b^*(\lambda_a)$ . For  $\lambda_a \gg 1$ , the system is almost full of prey ( $a \approx 1$ ) and, in some sense, the dynamics of the predators is close to that of the CP model. The predators die at rate 1 and spread at rate  $\lambda_b$ , but they cannot enter into the empty sites. One can introduce an effective  $\tilde{\lambda}_b$  and describe the process as a CP model, namely, the predators can enter any neighboring site at this rate. As the number of empty sites is proportional to leading order to  $1/\lambda_a$ , the effective

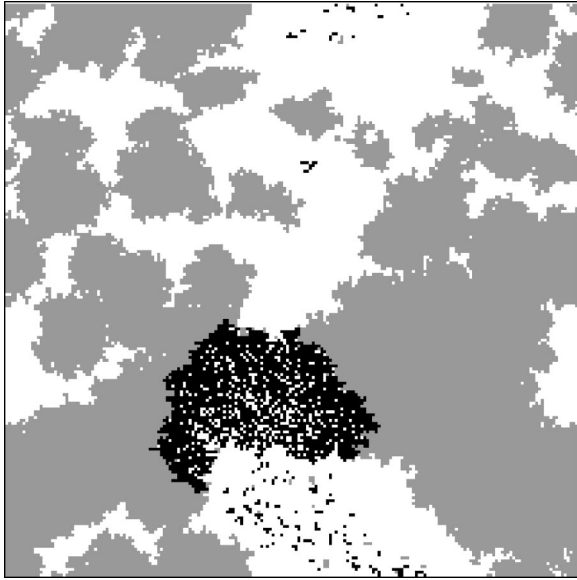


FIG. 12. Typical stationary state configuration of prey (grey) and predators (black) on a  $200 \times 200$  lattice at  $\lambda_a = 0.9$  and  $\lambda_b = 100$ . The white parts represent the empty sites. The picture shows the beginning of the invasion of the pure prey territory by predators, which were screened by empty sites before.

parameter should be  $\tilde{\lambda}_b = \lambda_b - c/\lambda_a$ , where  $c$  is a fitting parameter. As this CP model displays a phase transition at  $\tilde{\lambda}_b = \lambda_{CP}^*$ , in terms of the original parameter the transition occurs at  $\lambda_b^*(\lambda_a) = \lambda_{CP}^* + c/\lambda_a$ . This conjecture is in excellent agreement with the simulation data for  $\lambda_a > 0.5$  with  $c = 1.28(3)$  (see Figs. 1 and 3).

For  $\lambda_b \gg 1$ , new prey sites are usually immediately occupied by predators. However, with a small but finite probability, a predator site can disappear before the predators spread to the newborn prey site, and in this way, a prey site can be left alone to grow (similarly to the Eden model [24]). This rare event is negligible when the predator density is large enough and a prey island cannot grow for long periods of time. Practically this is the case for  $\lambda_a > \lambda_{CP}^*$ . In this case, the number of prey sites is negligibly small, and the predator sites behave as infected species in the CP model. One can see, in Figs. 7 and 8, that for  $\lambda_b = 100$  the two densities ( $a \approx b$ ) are equal to that of the CP model if  $\lambda_a > \lambda_{CP}^*$ . However, in the vicinity of  $\lambda_{CP}^*$  the densities are low, which allows an isolated prey island to grow for a long time. If  $\lambda_a < \lambda_{CP}^*$  the predator islands are shrinking, and, if  $\lambda_a$  and  $L$  are not too small, they can survive until a growing prey island reaches one of them. At this moment, the predators invade very quickly the prey territory and increase their population size (see Fig. 12). These new predator sites start to die out, leaving a few prey sites alone, and the whole procedure starts again. This mechanism insures the survival of the predators much below the CP critical density, and results in oscillations in the population sizes.

For  $\lambda_b > \lambda_b^T$ , but not too large, the qualitative picture is slightly different. As one can observe in Fig. 13, groups of predators are wandering through the system toward prey-

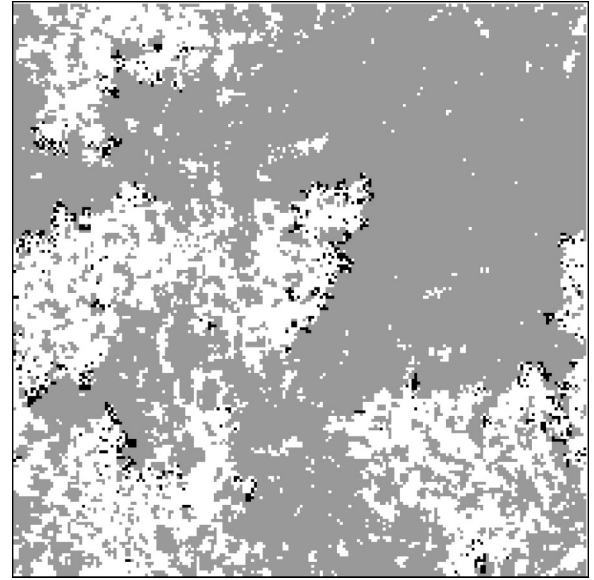


FIG. 13. The same as Fig. 12, but for  $\lambda_a = 0.2$  and  $\lambda_b = 5$ . Note that the predators invade only the fully dense prey areas in both figures.

dense areas. If two fronts of predators meet they usually stop moving, and the local population of predators starts to shrink. The oscillations are maintained in a somewhat similar way than for the  $\lambda_b \gg 1$  case: these predators can only survive if the prey become dense around them. This is more probable for larger values of  $\lambda_a$ , and it is also clear that the predators have a better chance to survive in larger systems.

According to the above statements, the key point in the underlying mechanism of oscillations is the existence of blocked predator islands which are located and trapped in sparse prey areas. Indeed, blocked predators in sparse prey areas result in growing prey populations; however, the resulting dense prey population allows predators to move and predate again. This mechanism drives back the system to the beginning of the loop. Clearly, predators can only be trapped in sparse prey areas if  $\lambda_a$  is smaller than or of the order of the death rate, 1. This explains the location of the oscillatory region. Note that the above argument is based on the spatial nature of the system, suggesting that a spatially extended character is fundamental for the existence of such prey-predator type of oscillations.

This mechanism also provides a qualitative understanding of the key properties of the system. The trapped predators can invade the prey area only when the prey are dense enough again, which takes a time proportional to  $1/\lambda_a$ , and leads to  $\omega \sim \lambda_a$ . According to simulations the correlation length  $\xi$  increases with decreasing  $\lambda_a$ . Indeed, as  $\lambda_a$  decreases, the trapped predators have to wait longer to escape; hence fewer groups of predators survive. This increases the distance between the groups, resulting in larger prey islands, whose average size is proportional to  $\xi_a$ .

When the correlation length is of the order of the system size, there are islands of prey of typical size  $L$ , extruding the predators out of the system. Hence the condition  $\xi_a \sim L$  characterizes the phase boundary between the oscillatory and

prey phases. On the other hand, a correlation length of order 1 ( $\xi_a \sim 1$ ), means that the noise dominates the system. Thus  $\xi_a \sim 1$  characterizes the boundary between the oscillatory and nonoscillatory regions of the coexistence phase.

As shown by the study of the time dependent correlations, domains separated by a distance larger than  $\xi_a$  oscillate asynchronously around a constant value with the same frequency,  $\omega(\lambda_a, \lambda_b)$ . According to this picture, one can derive a more quantitative description for the oscillatory region. Let us assume that, for  $1 \ll \xi_a \ll L$ , the global densities of each species can be written as the sum of local coarse-grained densities at a typical length scale  $\xi_a$ . Moreover, we assume that all these local densities oscillate with the same frequency but a different phase  $\alpha_l$ . In general, the amplitude of the local oscillations should depend on the parameters  $\lambda_a$  and  $\lambda_b$ . However, as one can observe in Figs. 12 and 13, the predators can only enter an almost fully dense prey area, and the predator fronts leave an almost empty field behind them. Hence, as suggested by the numerical simulations, everywhere in the oscillatory region, the local amplitude for the prey density can be considered as a constant,  $d$ . Thus

$$a(t) = a^s + d \left( \frac{\xi}{L} \right)^2 \sum_{l=1}^{(L/\xi)^2} \sin(\omega t + \alpha_l). \quad (22)$$

Supposing that the  $\alpha_l$  values change much more slowly than  $\omega$ ,  $a(t)$  shows a simple sine behavior for long periods of time (see Fig. 4). Thus, for  $a(t)$ , one can derive the value of the density fluctuations  $\chi_a$ , and the amplitude of these oscillations,  $A_a$ , using Eqs. (11) and (19), and take the average over all the possible  $\alpha_l$  configuration taken from a flat distribution. This procedure reproduces the result of Eq. (20) up to a multiplicative factor in front of the correlation length.

## VI. CONCLUSIONS

We have studied a two-dimensional prey-predator model (size  $L \times L$ ), which exhibits a rich stationary state phase dia-

gram. Particular attention has been paid to the study of finite size effects, and we were able to draw clear cut conclusions concerning the behavior of the model both for finite  $L$  as well as for the limit  $L \rightarrow \infty$ .

Three kinds of stationary states can be reached according to the values of the control parameters: a pure prey state, and two coexisting prey-predator ones, with and without oscillations. Two different kinds of second order transitions were found. Besides the usual DP transition we found a surprisingly different type of transition to the prey absorbing phase. The study of the global density fluctuations allowed us to characterize the crossover between the oscillatory and nonoscillatory domains of the coexistence phase. The distinction between these two domains remains valid in the infinite size limit. In the oscillatory regime, scaling relations were established between several physical quantities.

A qualitative explanation for the existence of such an oscillatory regime is given, pointing out the crucial role of the spatial extension of the system. Indeed, the frequency of the oscillations is determined locally due to the dynamics related to blocked predator islands in sparse prey areas. Regions of linear size  $\xi_a$  oscillate with the same frequency but with different phases. This explains the decreasing amplitude of oscillations with increasing system size. On the other hand, slowly changing phases result in periodic oscillations of the overall prey density for long periods of time. Moreover, for suitable choices of the control parameters one can have synchronized oscillations with finite amplitude across arbitrary large systems. Thus we think that our simple model could offer a qualitative explanation to the lynx population problem described in Sec. I.

## ACKNOWLEDGMENTS

We thank Z. Racz and G. Szabo for helpful discussions. This work has been partially supported by the Swiss National Foundation and the Hungarian Academy of Sciences (Grant No. OTKA T 029792).

- 
- [1] A. J. Lotka, Proc. Natl. Acad. Sci. U.S.A. **6**, 410 (1920).  
 [2] V. Volterra, *Leçons sur la Théorie Mathématique de la Lutte Pour la Vie* (Gauthier-Villars, Paris, 1931).  
 [3] N. S. Goel, S. C. Maitra, and E. W. Montroll, *Nonlinear Models of Interacting Populations* (Academic Press, New York, 1971); J. Hofbauer and K. Sigmund, *Evolutionary Games and Population Dynamics* (Cambridge University Press, Cambridge, 1998).  
 [4] B. Blasius, A. Huppert, and L. Stone, Nature (London) **399**, 354 (1999), and references therein.  
 [5] C. Elton and M. Nicholson, J. Anim. Ecol. **11**, 215 (1942).  
 [6] P. Rohani, R. M. May, and M. P. Hassell, J. Theor. Biol. **181**, 97 (1996).  
 [7] *Modeling Spatiotemporal Dynamics in Ecology*, edited by J. Bascompte and R. V. Solé (Springer, New York, 1998); *Spatial Ecology*, edited by D. Tilman and P. Kareiva (Princeton University Press, Princeton, 1997); *Metapopulation Biology*, edited by I. Hanski and M. E. Gilpin (Academic Press, New York, 1997).  
 [8] V. A. A. Jansen, Oikos **74**, 384 (1995).  
 [9] A. T. Bradshaw and L. L. Moseley, Physica A **261**, 107 (1998).  
 [10] J. E. Satulovsky and T. Tomé, Phys. Rev. E **49**, 5073 (1994).  
 [11] N. Boccara, O. Roblin, and M. Roger, Phys. Rev. E **50**, 4531 (1994).  
 [12] A. Provata, G. Nicolis, and F. Baras, J. Chem. Phys. **110**, 8361 (1999).  
 [13] K. Tainaka, J. Phys. Soc. Jpn. **57**, 2588 (1988); G. Szabo, M. A. Santos, and J. F. F. Mendes, Phys. Rev. E **60**, 3776 (1999).  
 [14] A. Pekalski and D. Stauffer, Int. J. Mod. Phys. C **6**, 777 (1998).  
 [15] A. Lipowski, Phys. Rev. E **60**, 5179 (1999).  
 [16] A. Lipowski and D. Lipowska, Physica A **276**, 456 (2000).  
 [17] B. Chopard, M. Droz, and S. Galam, Eur. Phys. J. B **16**, 575 (2000).

- [18] T. E. Harris, *Ann. Prob.* **2**, 969 (1974); T. M. Liggett, *Interacting Particle Systems* (Springer, New York, 1985).
- [19] M. J. Keeling and D. A. Rand, in *From Finite to Infinite Dimensional Dynamical Systems*, edited by P. Glendinnig and J. Robinson (Kluwer, Amsterdam, 2000).
- [20] W. Kinzel, in *Percolation Structures and Concepts*, *Annals of the Israel Physical Society* Vol. 5 (Adam Hilger, Bristol, 1983), p. 425; P. Grassberger, *J. Phys. A* **22**, 3673 (1989); J. Marro and R. Dickman, *Nonequilibrium Phase Transitions in Lattice Models* (Cambridge University Press, Cambridge, 1999).
- [21] H. K. Janssen, *Z. Phys. B: Condens. Matter* **42**, 151 (1981); P. Grassberger, *ibid.* **47**, 365 (1982).
- [22] A. Rozenfeld and E. Albano, *Physica A* **266**, 322 (1999).
- [23] R. Monetti, A. Rozenfeld, and E. Albano, *Physica A* **283**, 52 (2000).
- [24] M. Eden, in *Symposium on Information Theory of Biology* (Pergamon Press, New York, 1958).